Visualization of Particle Interactions in Granular Media

Holger A. Meier, Michael Schlemmer, Christian Wagner, Andreas Kerren,
Hans Hagen, Ellen Kuhl, and Paul Steinmann

Abstract— Interaction between particles in so-called granular media, such as soil and sand, plays an important role in the context of geomechanical phenomena and numerous industrial applications. Proposing a two scale homogenization approach, a micro and a macro scale level are introduced. The behavior of the granular matter on the micro scale level is captured by a discrete element method, allowing the simulation of breaking and forming of contacts between the single grains. The problem on the macro scale level is discretized by the finite element method. Computation of granular material in such a way gives a deeper insight into the context of discontinuous materials and at the same time reduces the computational costs. However, the description and the understanding of the phenomena in granular materials are not yet satisfactory and a sophisticated problem specific visualization technique would help significantly to illustrate failure phenomena on the microscopic level. In this paper, we present a novel 2D approach for the visualization of simulation data, based on the above outlined homogenization approach. Our visualization tool supports visualization on the micro scale level, based on a discrete element method, as well as visualization on the macro scale level, discretized by finite elements. Interactive rose diagrams are used, representing the dynamic contact networks on the micro scale level in a condensed and efficient way. The tool shows both aspects closely arranged in form of coordinated views to give users the possibility to analyze the particle behavior effectively.

Index Terms—Visualization, mechanics, granular media, particle interaction.

1 Introduction

Multiscale simulation is currently one of the most promising fields of research in geomechanical engineering since it is known to combine efficiency and robustness of macro scale level simulations with accuracy and preciseness of micro scale level analyzes. In the present manuscript, we shall outline our recently developed *two-scale simulation tool* for granular media and illustrate the need for a corresponding *two-scale visualization tool*. On the macroscopic level, our approach utilizes a finite element method to allow for efficient and robust large scale engineering computations. The finite element method is essentially based the continuum hypothesis, i.e., it implies that matter is distributed continuously in space and can be characterized rigorously through a set of field equations in terms of continuous quantities. When thinking of granular media such as sand and powders it is quite obvious that these can hardly be characterized as continuous. Accordingly, in order allow for a more precise representation, we *zoom in to the microscopic simulation* where matter is inherently discontinuous. On this second scale, simulations are performed with the discrete element method which essentially evaluates particle-to-particle interactions. Obviously, a discontinuous technique like the discrete element method is able to represent discrete failure phenomena such as crack propagation more accurately than continuous strategies.

Although research in the area of *multiscale simulation* has been quite intense within the past decade, there is hardly any progress in corresponding fields such as *multiscale visualization*. From an engineering point of view, multiscale visualization tools which allow to *zoom in to the microscopic visualization* would significantly improve the understanding of complex failure phenomena and maybe even support the development of new, more sophisticated material models.

Although individual visualization tools are available for the continuous macroscopic and for the discontinuous microscopic level, there is still no unique visualization tool that provides a linkage between these two scales. Macroscopic visualization which is typically based on relevant scalar-, vector- and tensor fields has been solved quite satisfactorily from an engineering point of view. Microscopic visualization, however, is still in its infancy and commonly restricted to providing an overview of the particle structure. The efficient combination of both macroscopic an microscopic visualization tools is usually hampered by non-compatible data structures.

The present research project aims at identifying novel visualization methods for the microscopic level with the ultimate goal of deriving a multiscale visualization tool capable of providing a combined view of both levels of multiscale computation. In this context, we analyze the applicability of the traditional rose diagram visualization to provide additional microscopic information about force networks in granular media. This technique from Information Visualization is applied to data arising from the micro scale level analysis. Accordingly, our work also implies a linkage between SciVis and InfoVis. The rose diagram enables a selective visualization of force directions, revealing structures and offering new points of view for the engineer to efficiently analyze large data sets resulting from the granular simulation. For the generation of the rose diagrams itself a specific sweepline algorithm is introduced to process the data sets, including an adapted cluster algorithm to produce numerically stable rose diagrams, even for large amounts of data.

Both simulation tools, the finite element method and the discrete element method provide time dependent data sets which manifest themselves in individual load steps. The sequence of load steps on the macro and micro scale level can be animated or controlled by a *VCR-metaphor*.

This manuscript is organized as follows: Section 2 will present a brief summary of the homogenization process from an engineer's point of view. Related work for both, mechanics aspects, as well as visualization aspects will be presented in Section 3. Our visualization system and techniques for the micro and macro scale level will be illustrated in Section 4, while details of the implementation are revealed in Section 5. Finally, representative results are discussed followed by

- *Holger A. Meier and Paul Steinmann, Department of Mechanical and Process Engineering, University of Kaiserslautern, Germany, E-mail: {homei | ps}@rhrk.uni-kl.de.*
- *Michael Schlemmer, Christian Wagner, and Hans Hagen, Department of Computer Science, University of Kaiserslautern, Germany, E-mail: {schlemmer | hagen}@informatik.uni-kl.de and wagners-christian@web.de.*
- *Andreas Kerren, School of Mathematics and Systems Engineering, Växjö University, Sweden, E-mail: kerren@acm.org.*
- *Ellen Kuhl, Department of Mechanical Engineering, Stanford University, USA, E-mail: ekuhl@stanford.edu.*

Manuscript received 31 March 2007; accepted 1 August 2007; posted online 2 November 2007.
For information on obtaining reprints of this article, please send e-mail to: tvcg@computer.org.

a conclusion and ideas for future improvements.

2 BACKGROUND

Provided in the following is a brief overview regarding the mechanical procedures. Keeping in mind that the focal point of this contribution is found in the visualization of data sets originating from multiscale computations, containing a macro and a micro scale level, deeper insight of the related mechanics is found in the literature in the references. In particular, the visualization finds its main attention on the micro scale level, see Subsection 4.2.

The *two scale homogenization*, closer observed in Subsection 2.1, incorporates a finite as well as discrete element approach. A standard *finite element method* (fem) is utilized on the macro scale level, assuming an overall homogeneous and continuous material. Each point on the macro scale level is related to a micro structure. The micro structure under consideration is assumed to be heterogeneous as well as discontinuous, modeled by a *discrete element method* (dem). Due to the focus of this manuscript, the homogenization approach and the micro scale level computation are outlined in Subsection 2.1 and 2.2. Despite the importance of the finite element approach, we will not address the theme of finite element computation in detail. Rather, we refer the interested reader to standard finite element literature. The complete homogenization cycle is depicted in Fig. 1.

2.1 Two scale homogenization approach

Modeling and simulation of confined granular medium includes the description of the behavior of single grains as well as grain groups. The advantages of homogenization schemes are found in the capability to project microscopic quantities onto macroscopic behaviors. Thereby, in our case, the microscopic level shows the true structure of the granular media $\mathscr{G}$, consisting of an arbitrary arrangement of grains, see Fig. 1 (lower left). Such approaches allow to convey the distinction of dry granular matter, i.e., the ability to form and break contacts between the single grains. This feature is of great importance since forces inside granular media are solely transmitted at contact points. Note, due to the arbitrary arrangement of the grains inside, quantities inside the granular assembly vary strongly over the domain of interest. Nevertheless, the theorem of HILL [13] states: the mechanical power on the macro scale level has to be equivalent to the averaged mechanical power on the micro scale level.

$$\overline{\boldsymbol{P}} \,\vdots\, \dot{\overline{\boldsymbol{F}}} = \langle\, \boldsymbol{P} \,\vdots\, \dot{\boldsymbol{F}} \,\rangle = \langle\, \boldsymbol{f}_{ij} \bullet \dot{\boldsymbol{l}}_{ij} \,\rangle \tag{1}$$

Therein, quantities holding an over bar are associated with the macroscopic scale, whereas quantities without are related to the micro scale level. Both, the PIOLA tensor $\boldsymbol{P}$, see MALVERN [15], as well as the material velocity gradient tensor $\dot{\boldsymbol{F}}$ are considered to be two field tensors, i.e., standing between the initial and the current configuration, see Fig. 1. The branch vector $\boldsymbol{l}_{ij}$ between the particles i and j is defined as the vector connecting the particle centers, whereas $\boldsymbol{f}_{ij}$ represents the contact force between the particles i and j. Superimposed dots on quantities point out the derivative with respect to the time. For the sake of simplicity, we will omit the definition of the volume average procedure, denoted by $\langle\bullet\rangle$, and refer the interested reader to the publications [13, 17, 20]. Using (1), fluctuations on the micro scale level are smeared over the microscopic domain. The HILL theorem builds the fundament of most homogenization procedures and is used to link averaged microscopic to macroscopic quantities. Additional, HILL's theorem leads to a choice of an appropriate *representative volume element* (rve).

A geometric periodic rve, i.e., a periodic sample of the material of interest, which is large enough to capture all effects of the true material and small enough to be representative for the entire micro structure of the domain of interest on the micro scale level, is laid out. Note that we assume a geometric periodicity with the period equal to the length of the rve itself, see Fig 2. Comparing the scale of the macro structure L with the micro structural scale l we demand a length on the micro scale level to be significantly smaller than a length on the macro scale level, i.e., $l \ll L$.

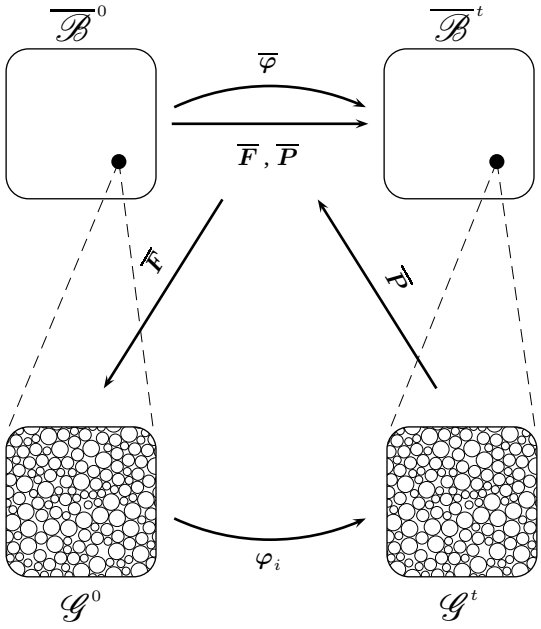

Fig. 1. Illustration of the two scale homogenization. The upper left quarter shows the macroscopic body in the reference configuration $\overline{\mathscr{B}}^0$ at time zero. The macroscopic body in the current configuration $\overline{\mathscr{B}}^t$ is depicted in the upper right quarter. Mapping between the reference and current configuration is accomplished by the macroscopic non-linear deformation map $\overline{\boldsymbol{\varphi}}$. The granular micro structure $\mathscr{G}^0$ at time zero is found in the lower left quarter, whereas the current micro structure $\mathscr{G}^t$ at time t is found in the lower right corner. The mapping between the configurations of the granular micro structure is based on the microscopic non-linear deformation map $\boldsymbol{\varphi}_i$. Applying the macroscopic deformation gradient tensor $\overline{\boldsymbol{F}}$ to the granular micro structure results into a stress response $\overline{\boldsymbol{P}}$, resembling the PIOLA stress.

An effective algorithm to produce ab initio geometric periodic rves has been introduced by MEIER ET AL. [16], allowing the generation of rves by a given grain size distribution.

On the macro scale level, only the homogenized, i.e., averaged, effective material response is considered. Therefore, we can consider the material on the macro scale level to be homogenious, allowing the application of a continuum approach. In what follows, boundary conditions on the micro scale level are solely applied according to the TAYLOR model. Thus, we assume particle fluctuation inside and on the boundary of the rve to be zero.

2.2 Micro scale level computation

The mechanics on the micro scale level of our homogenization approach are based on the dem, introduced by CUNDALL AND STRACK [5] in the late seventies. They presented an explicit discrete numerical method to analyze the behavior of granular media. The dem allows the simulation of the behavior of granular matter in a natural way, yielding to equivalent results if compared to experimental data [4, 6]. Complicated behaviors, such as continuously non-linear stress/strain response, dilation related to mean stress, transition from brittle to ductile behavior, hysteresis and memory, as well as breaking and forming of contacts between the single grains automatically appear from the dem [3].

Please note, for the sake of simplicity, without a loss of generality of the visualization, we restrict this contribution to smooth particles. Thus, the tangential part of the contact force between the single grains is disregarded. Additionaly, we assume a dry particle assembly, ex-

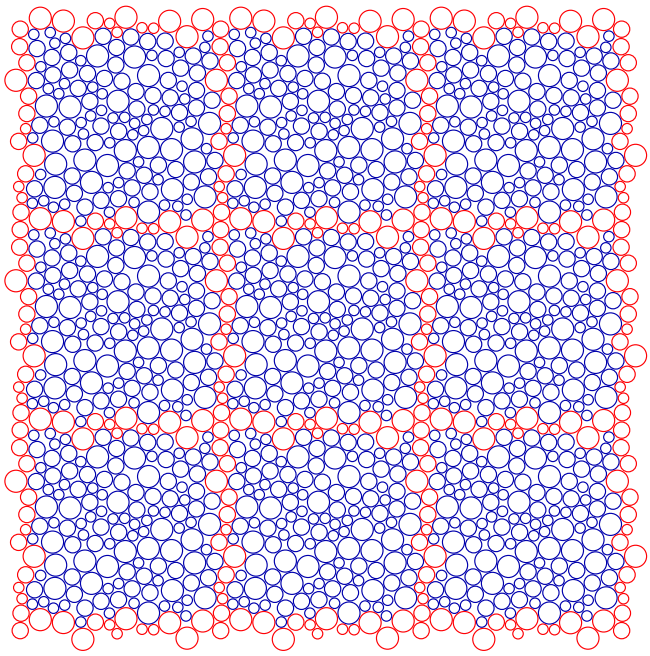

Fig. 2. Granular assembly showing nine geometric periodic cells. The period is measured between the centers of the red circles. The red circles generate the boundary of the geometric periodic rve and belong to the boundary particle set $\mathscr{B}$, where as the particles in the inner are associated with the inner particle set $\mathscr{I}$. Note, the choice of the geometric periodic rve is not unique.

cluding any kind of attraction forces.

In the case of dry granular media forces inside the granular assembly solely transmit at the contact points. Contact forces between the particles depend on a penalty force approach. The magnitude of the normal contact penalty forces depends on the overlap between the particles. The overlap ε_{ij} between the particles i and j is calculated by subtracting the particle radii from the length of the branch vector, yielding to: $\varepsilon_{ij} = \| \boldsymbol{l}_{ij} \| - \left[r_i + r_j \right]$. For the distance between the grains equal or larger to the sum of the particle radii, i.e., $\varepsilon_{ij} > 0$, the magnitude of the normal penalty force is set to zero. In the case of contact, i.e., the distance between the particles being less than the sum of their radii, the magnitude of the normal penalty force is calculated by a potential energy function ψ_n depending on the particle overlap. The normal contact force, unequal to zero for $\varepsilon_{ij} < 0$, is thermodynamically conjugated to the particle overlap ε_{ij}.

$$\boldsymbol{f}_{n,ij} = \psi_n' \left(\varepsilon_{ij} \right) \boldsymbol{n}_{ij} \tag{2}$$

Therein $\boldsymbol{n}_{ij}$ represents the contact normal, related to the branch vector by $\boldsymbol{n}_{ij} = \boldsymbol{l}_{ij} / \| \boldsymbol{l}_{ij} \|$. The prime on the energy function ψ_n denotes the derivative with respect to the overlap of the particles i and j.

Due to the application of the TAYLOR assumption, each single particle is mapped by the macroscopic deformation gradient tensor $\overline{\boldsymbol{F}}$. Thus, the position of particle i at time $n+1$ is calculated by

$$\boldsymbol{x}_i^{n+1} = \overline{\boldsymbol{F}} \bullet \boldsymbol{x}_i^0 . \tag{3}$$

The macroscopic deformation gradient tensor $\overline{\boldsymbol{F}}$ is understood as a map of the initial particle position $\boldsymbol{x}_i^0$ to the current particle position $\boldsymbol{x}_i^{n+1}$ at time $n+1$. Additionally, Eq. (3) identifies the macroscopic deformation gradient tensor as the driving quantity of the whole homogenization process, see Fig. 1. To complete the homogenization cycle as shown in Fig. 1, an averaged stress quantity needs to be returned to the macroscopic level. With regards to the mechanical power on the macro scale level we select the macroscopic PIOLA stress $\overline{\boldsymbol{P}}$ to be the quantity desired. The macroscopic PIOLA stress tensor results by the use of averaging theorems to

$$\overline{\boldsymbol{P}}^{n+1} = \langle \, \boldsymbol{P}^{n+1} \, \rangle = \langle \, \boldsymbol{f}_{ij}^{n+1} \otimes \boldsymbol{l}_{ij}^0 \, \rangle . \tag{4}$$

Thereby $\boldsymbol{P}$ states the microscopic PIOLA stress tensor, depending on the normal contact forces between the particles. Determination of the macroscopic PIOLA stress tensor completes the computation on the micro scale level.

3 Related Work

In the context of finite, as well as of discrete element computation most visualization tools are intrinsically combined with the computational tools, counting as software packages. Extentions or changes are limited when it comes to commercial software packages. The most prominent commerical software packages used in fem computations, among others, are ABAQUS [1] and ANSYS [2], whereas in the case of dem analysis, DEM Solutions [10] and software from Itasca [14] are to name. To the best knowledge of the authors, software does not exist which is capable to perfom the visualization, or the computation of multi scale problems including different computational approaches on each scale.

In this work we will present a modified visualization of the so-called *rose diagrams*. These diagrams, introduced by NIGHTINGALE [18], are commonly used for displaying circular information structures. The construction of our improved rose diagram is based on sweep line paradigms, known from computational geometry. An example for a similar application of this class of algorithms is the work of FORTUNE [11] on the computation of Voronoi diagrams. The book of DE BERG ET AL. [8] gives a good overview of the various application areas of this paradigm.

Our visualization method also incorporates a type of hierachical clustering, i.e., agglomerative clustering. A lot of work has been done based upon agglomerative clustering. The most relevant ideas, incorporated into our approach, are those of WARD [19], since a similar variance criterion is used in our clustering process. DAY AND EDELSBRUNNER [7] presented a range of optimized algorithms regarding this topic, including the algorithm of DEFAYS [9].

4 Visualization

While current visualization systems solely deal with either fem or dem visualization, our approach joins both, macro and micro scale level visualization. In our procedure we combine standard SciVis methods with enhanced InfoVis methods, resulting in a novel visualization possibility for data resulting from multiscale computations. Paralleling the simulation scheme (see Section 2) , the visualization scheme is divided in two main levels, the macroscopic and the microscopic one. The macro scale level view serves as a representation of the fem grid and offers standard visualization techniques for the common fem approach. Moreover, special previews for the underlying micro scale level have been introduced. For each gauss point, included in the fem mesh on the macro scale level, a link to the corresponding micro scale level view is available. Both levels contain time-variant data, partitioned into the so-called *load steps*. Hereby, one load step at macro scale level corresponds to multiple load steps on the micro scale level. The control of this time variation is accomplished by a *VCR-metaphor* introduced in both view levels. Each view level is described in the following. Furthermore, possible interactions between the visualization levels are specified.

4.1 Macro scale level View

The fem mesh as well as related features, e.g., bearings, forces, glyphs and gauss points, are displayed in the macro scale level view, see Fig 3. Bearings are represented by unfilled triangles. Arrows are used to visualize forces which act on the fem nodes. The direction of the forces is collinear to the arrow directions, while the magnitudes of the forces are resembled by the length of the arrows. The positions of the Gauss points, i.e., the locations where the microscopic constitutive equations are evaluated, are a standardized input to the finite element calculation.

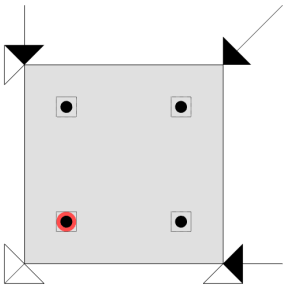

Fig. 3. Single finite element, containing a typical number of gauss points. The gauss points are displayed as black circles. Selected gauss points are highlighted, using a color scheme. Bearings are represented by unfilled triangles, while forces are idealized by arrows.

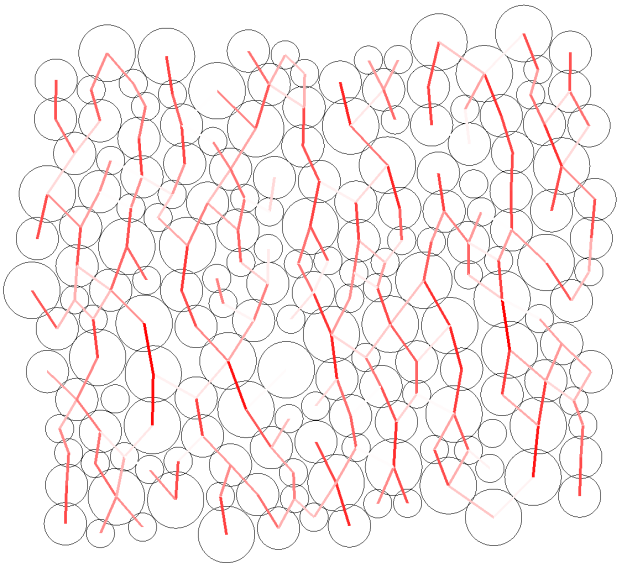

Fig. 4. Granular view of a single rve, edge representation. The particles are depicted as black bounded circles. The magnitude of the overlaps is visualized by a color coding scheme. Therefore, the branch vectors between the connecting particles are colored. Darker colors represent a deep penetration, while light colors are associated with a narrow penetration.

In the case of nonlinear discrete as well as finite element computation, loads and deformations are applied in multiple load steps, ensuring the convergence of the algorithm. These load steps can be thought of as pseudo time steps, controlled by a classical VCR-metaphor. Starting an animation on the macro scale level view relates to a corresponding synchronized animation of the micro scale level view. Connections between the macro and micro scale level view take place at the gauss points, which are depicted by black circles. Selected gauss points, leading to a view of the connected micro scale level structures, are highlighted. A color coding scheme, resulting to sober associations between the selected gauss points and the micro structures, is utilized. Glyphs, presenting features of the micro scale level view, e.g. rose diagrams or density functions, are superimposed on the belonging gauss points. These kind of features are part of the micro scale level view and are discussed in Subsection 4.2.

4.2 Micro scale level View

Visually evaluating the results of the particle computations, obtained by a dem on the micro scale level, is of great interest to researchers in the engineering community. Each gauss point belonging to the finite element mesh of the macro scale level contributes a set of visualization data, i.e., data that needs to be visualized on the macro scale level, see Subsection 4.1, as well as data, gained from the computations on the micro scale level at a particular gauss point, necessary to visualize on the micro scale level. Thus, in order to conquer the task of providing an adequate tool to visualize all relevant data, our tool provides a second view level. This second view level solely supplies views of microscopic data for selected gauss points.

Similar to the visualization procedure on the macro scale level, different load steps have to be visualized on the micro scale level. In detail, each load step on the macro scale level contains multiple load steps on the micro scale level. For the sake of familiarity, the VCR-metaphor, as presented in Subsection 4.1, is re-utilized for this task.

Color coding, relating gauss points of the finite element mesh on the macro scale level to the rve on the micro scale level, renders an easy and efficient identification, i.e., the frame color of the selected gauss points relates to the color of the box framing the rve. In each of these boxes two different views are available.

The first view, called *granular view*, shows the particles pictured as circles, see Fig. 4. The user can choose between a filled or edge representation. While the filled representation gives a good overall impression of the granular assembly, the edge representation emphasizes the overlaps between the grains. Additionally, the filled view shows the periodic boundary particles in a different color. The overlaps, which out-stand in the edge representation, are of great importance, see Subsection 2.2. Their magnitude is directly related to the contact normal force acting between the particles in contact and effect the particle displacement. The GUI allows a fast change between the so called *overlap mode* and the *normal view mode*. Another feature of the granular view consists of the possibility of showing the particle contact network. During the overall computation single particles as well as particle groups move inside the bounded rve, yielding to new particle arrangements as well as contact networks. Visual inspection includes the analysis of connection lines, running through the particle assembly, the appearance and disappearance of voids inside the granular structure. In the granular view, the user can opt for showing connection lines. These lines also enclose voids and non-connected particles, while their main feature is based in resembling the contact connectivity between the grains. Moreover, the user can observe the magnitude of the normal contact forces by enabling a color mapping of this feature onto the drawn connection lines. Thereby, darker lines indicate greater magnitudes of the normal contacts forces.

The second view, titled *diagram view*, shows a *rose diagram*. The rose diagram, originally introduced by NIGHTINGALE [18] in 1858, offers a two-dimensional graphical representation of discrete and discretized circular data. In its definition, the classical rose diagram relates to a modified version of a histogram. Thereby, histogram bars correspond to the tiles of the rose diagram. The main difference between the rose diagram and the histogram is found in the intrinsically periodic data representation of the rose diagram. We use an enhanced type of rose diagram, laid out in Section 5, to represent the directions of contact between the touching particles. Depending on the deformed rve, including the changed particle setup inside, a distinguishing load transfer direction inside the granular structure might be found. This load transfer direction is well analyzed by the rose diagram representation, while in the granular view a clear analysis might be unmanageable. The degree of refinement, i.e., the number of desired segments, can be arbitrarily determined by the user. A scanline algorithm, see Subsection 5, is applied to construct the diagram itself. Basically, a delta region around an angle is observed. The appearances of angles in this delta region are counted and represented as blossoms. Thin equispaced radial lines around the diagram center have been added for a better visual comparison of blossom length in the diagram itself, as

well as for comparison among different load steps or data sets.

The most relevant feature of our tool is its ability to interact straightforwardly between the rose diagram representation and the granular view, i.e., both features are linked together. Besides the ability of transforming the shape of the rose diagram by adjusting the scanning parameters, it is possible to select parts of the diagram. Selecting a part of the rose diagram highlights contacts inside the granular view, collinear to the selected segment of the rose diagram. This filtering feature enables the user to directly observe the internal contact directions, which relate to the selected segment of the rose diagram and can be utilized in any load step to reveal directional shifts.

In addition to the rose diagram, the diagram view offers the possibility of showing a density representation. One can regard this *density diagram* as a rose diagram including an infinite number of tiles. The density diagram depends only on the delta region, used to count the contact angles. A wider delta angle will lead to a smoother representation, while a very small delta angle will lead into a very rough high frequency signal. The choice of this angle is not obvious for varying data sets. Therefore, the density diagram can be used to visually determine an appropriate delta angle for rose diagrams. Using fixed angles or fixed frequency spectra, one could extract the border of the density diagram to perform shape comparisons.

5 Implementation Aspects

The overall key aspects of the presented visualization tool are found in the capability to handle and visualize data sets resulting from multiscale computations. In general, these kind of computations produce a large amount of structured data, separated in multiple files. In our case, data is ordered by index triples, comprised of macro load steps (mls), elements (elem), as well as gauss points (gp), leading to a number of files equal to: nof $=$ mls $*$ elem $*$ gp. Thus, handling of the files itself results in an interesting challenge.

Each file contains macroscopic data, e.g., stress tensors, associated with the index triple. Furthermore, each file contains data of the micro scale level computation, e.g., particle positions, partitioned by microscopic load steps. The number of microscopic load steps differs in each file, depending on the applied deformation.

The amount of current data, as well as the intention of a three dimensional extension calls for an efficient programming language and a rapid visualization framework. Hence, implementation is performed by C++, Qt and OpenGL.

The visualization key aspect on the micro scale level relates to a novel procedure for rose diagram construction. In the present case, data for a rose diagram arises from the unit contact normal vectors $\boldsymbol{n}_{ij}$. A unit contact normal vector $\boldsymbol{n}_{ij}$ results from the normalized branch vector $\boldsymbol{l}_{ij}$, which connects the centers of the particles i and j. Due to the ambiguousness of the unit contact normal vectors $\boldsymbol{n}_{ij}$ and $\boldsymbol{n}_{ji}$, respectively, rose diagrams of granular media are intrinsically point symmetric. Please note, each unit contact normal vector can be thought of as an angle inside polar coordinate system.

Traditionally, rose diagram construction follows a simple but error-prone procedure. First, a circular domain is partitioned into equal sized segments. Afterwards, the unit contact normal vectors are related to the appropriate segment of the circular domain, by comparing the contact normal angle with the circle segments. Counting the number of contact normal angles related to each segment equates the segment radius. A normalization of the segment radii closes the classical rose diagram construction. In particular cases, classical rose diagram construction leads to unexpected outcomes, relating to numerical errors in the underlying data, see Fig. 5.

Our rose diagram construction prevents such errors by keeping the segment width variable. Therefore, we convert the set of appearing contact normal angles into a function defined on the angular continuum. Introducing the region of influence, defined by s, leads to a definition of the directional density ρ. For an arbitrary angle α, the region of influence boundaries are defined as $a = \alpha - s/2$ and $b = \alpha + s/2$, respectively and border the right open interval $[a, b)$.

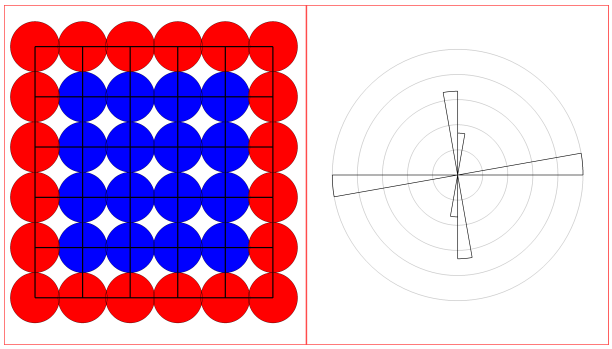

Fig. 5. Particle assembly with corresponding classical rose diagram. Visualization errors, originating from numerical errors, are visible.

$$\rho\ (\alpha\ ) = \frac{1}{s} \sum_{i} \chi_{[a,b)} \left(\angle \left(\boldsymbol{e}_1 , \boldsymbol{n}_{ij} \right) \right) \tag{5}$$

Therein, the angle by a direction $\boldsymbol{n}_{ij}$ influences the density function ρ if and only if α lies in the region between $k = \angle \left(\boldsymbol{e}_1 , \boldsymbol{n}_{ij} \right) - s/2$ and $l = \angle \left(\boldsymbol{e}_1 , \boldsymbol{n}_{ij} \right) + s/2$, respectively. Therefore, the density function ρ is a piecewise constant function, constructed by a sum of rectangle impulse functions, whereby each rectangle impulse function results from the corresponding direction $\boldsymbol{n}_{ij}$, bounded by k and l. The paradigm of sweep line algorithms is commonly used in computational geometry. Our sweepPie-algorithm is based on collecting data related to the contact normal angles. Therefore, an angle segment of size s is positioned twice for each direction, once in the case of an inEvent and once in the case of an outEvent. An inEvent, see Fig. 6, left, is defined by positioning the left side of the angle segment onto the angle. In this case, the associated angle α_{in} is defined by $\alpha_{\text{in}} = k$. Placing the right side of the angle segment onto the angle defines the outEvent, see Fig. 6, right. Thereby, the associated angle α_{out} yields $\alpha_{\text{out}} = l$. The number of angles, corresponding to $\boldsymbol{n}_{ij}$, inside the

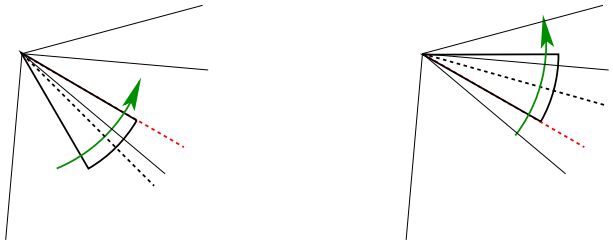

Fig. 6. Illustration of the inEvent and the outEvent. The left side of the figure shows the inEvent for a contact normal vector $\boldsymbol{n}_{ij}$, marked by the red dashed line, with its corresponding angle α, marked by the black dashed line. The right side shows the outEvent to the same normal vector $\boldsymbol{n}_{ij}$. The associate size of the angle segment is defined by s.

angle segment is counted and stored. Processing all occurrences by sorting them in increasing order with respect to the associated angle results in the density function ρ, depicted in Fig. 7. A corresponding rose diagram, see Fig. 8, results from the latter described density function ρ by using a clustering algorithm. In detail, the neighboring constant density function intervals, containing the smallest variance, are combined. Thus, for a number of finite combinations the proposed density function reaches a constant value and is represented by a single segment. In our case, a full distance matrix, resulting from the distance metrics of neighboring cluster segments, is unnecessary. This conclusion results from the fact that each segment has only two neighbors.

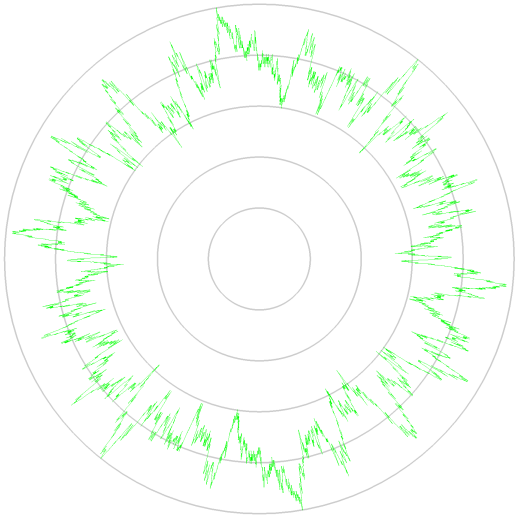

Fig. 7. Piecewise constant density function of an statistically isotropic sample. The corresponding rose diagram is depicted in Fig. 8.

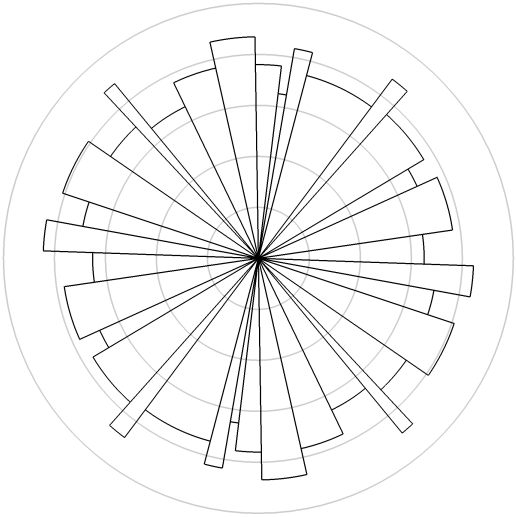

Fig. 8. Resulting rose diagram after clustering of the density function shown in Fig. 7.

Formally, the distance to all other segments is ∞. In consequence, calculation of clustered rose diagrams is not limited by the number of particle contacts. This arises from the fact that neighboring information can be found and updated in $\mathcal{O}(1)$. Due to the fact that there are always two segments which form one new clustered segment, runtime and memory usage are of order $\mathcal{O}(n)$.

6 Results

We have applied our visualization tool to a well-known problem from the area of geomechanics. This problem consists of a footing being pressed into the soil ground. The deformed structure is seen in Fig. 9. The overall soil on the macro scale level is discretized by 40 finite elements. Note, due to the symmetry of the problem considered, only one half of the complete problem is modeled. Each finite element contains 4 gauss points. The procedure of pressing the footing into the soil ground is modeled by prescribing the deformation of three nodes of the finite element mesh. The total deformation is applied in 100 load steps.

Each gauss point is related to one rve on the micro scale level, resulting into a total number of 160 rves. Each rve contains 182 grains and is generated with the algorithm proposed in [16].

The visualization of the solution data of the latter described geomechanical problem is impressive. Glyphs on the macro scale level view give a good overview of the related contact network inside the associated rve on the micro scale level view. Thus, identification and analysis of certain quantities of interest is done in a minimum of time. In Fig. 9 four gauss points of special interest are selected on the macro scale level view according to their rose glyph representation and can in parallel be analyzed in further detail on the micro scale level view, Fig. 10. The visual link between macro and micro scale level is supported by usage of corresponding color frames. Additionally, the capability of one tool handling all the data resulting from multiscale computations leads to an enormous work reduction. On the micro scale level, the novel approach of visualizing contact network data yields into a total success, based on the variable and unfixed segments. Interaction features, relating the segments of the rose diagram to the corresponding contacts inside the rve, turn out to be a great help in analyzing the load carrying behavior of granular materials, see Fig. 10. Furthermore, the novel formulation of the rose diagram excludes influences based on the numerical errors of the visualization data.

7 Conclusion

We have presented a new system for interactive visualization of a two scale homogenization process. The novel combination and connection of both views, namely the finite element method (fem) view and the advanced discrete element method (dem) view, helped to improve research in the area of Geomechanical Engineering. Besides the implementation of standard visualizations, we have introduced a new class of rose diagrams for the purpose of visualizing force directions on micro scale level (dem) view. Interaction with these novel diagrams, enables selective visualization of force direction patterns in the granular media. This shows relevant contacts inside the load carrying network, making our system an important new tool for further research in this area. The cluster algorithm, used for the rose diagram generation, takes advantage of the segment neighborhood structure so that it is suitable for large data amounts.

In future work, we plan to improve performance especially for the computation of the connectivity network for faster loading of data sets. Since parameter adjustments for density computations still have to be determined manually by the user, we also plan to provide an adaptive parameter adjustment. Another challenge will be the development of further methods to transfer our technique to three dimensional data.

Acknowledgements

The authors thank the German Research Foundation (DFG) for financial support within the DFG International Research Training Group 1131, “Visualization of Large and Unstructured Data Sets – Applications in Geospatial Planning, Modeling, and Engineering” at the University of Kaiserslautern, Germany. We also like to acknowledge

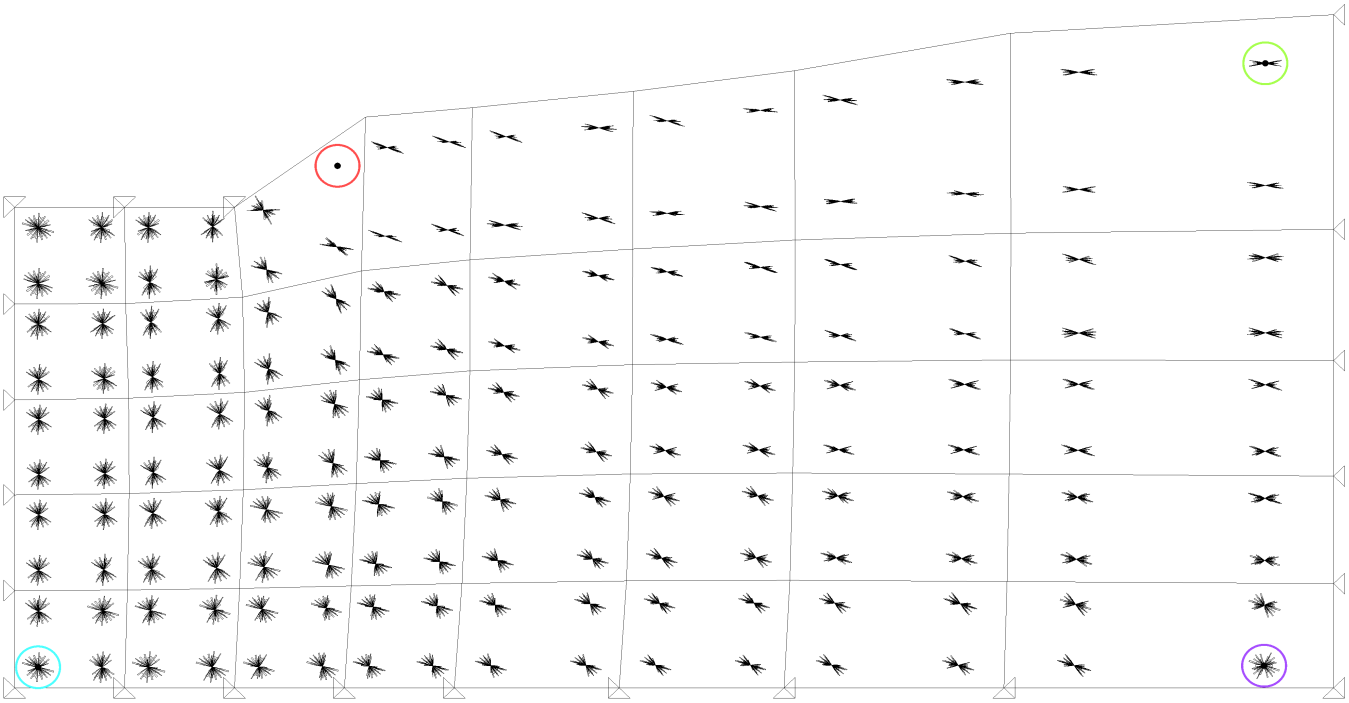

Fig. 9. Macro scale level view of the final deformed state. 40 finite elements are used to discretize one half of the footing problem. Boundary conditions are applied by displacements of the restricting bearings. Glyphs are visible and give a good expectation of the underlying micro structure. rves of the marked gauss points are depicted in Fig.10.

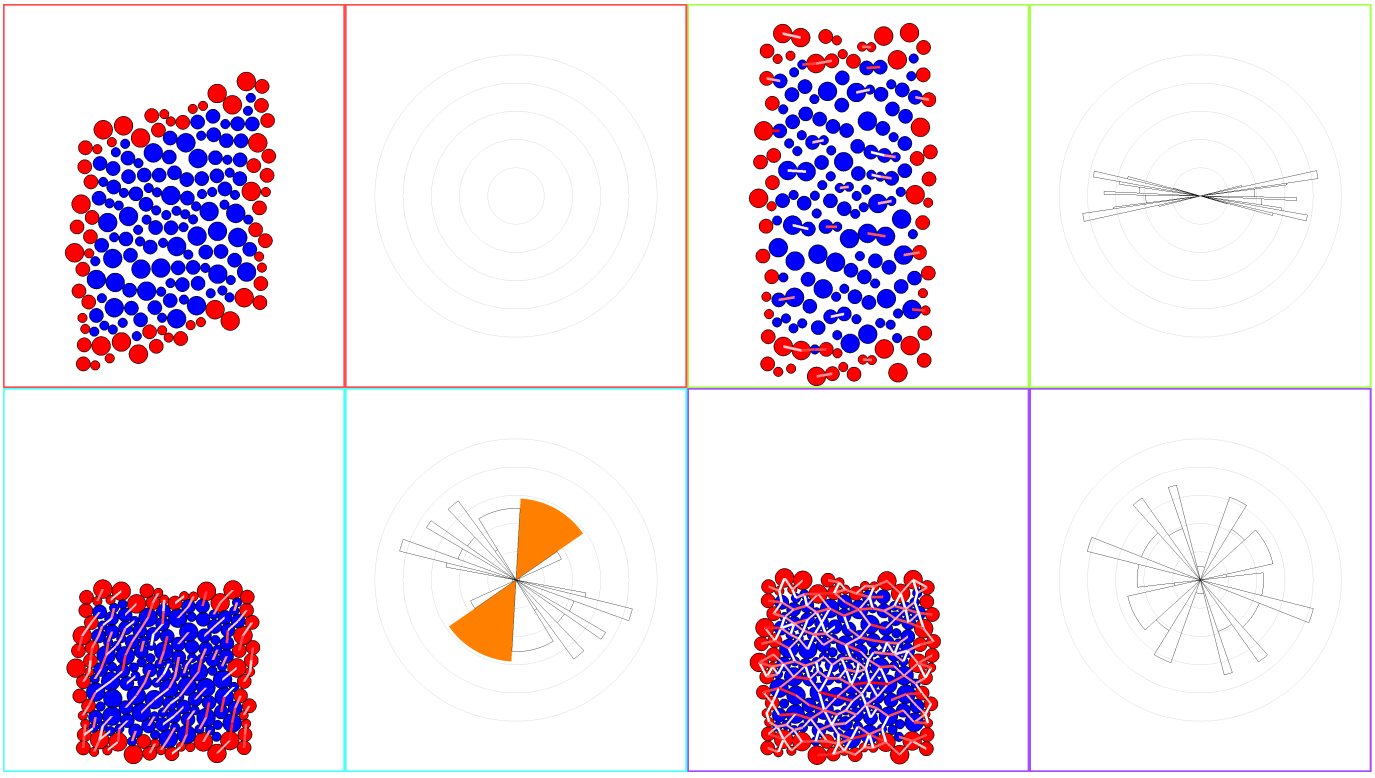

Fig. 10. Micro scale level view of four selected rves. Each pair, e.g., a particle assembly and the corresponding rose diagram, is related to one gauss point on the macro scale view level by its colored frame.

Burkhard Lehner, Computer Graphics and Visualization, University of Kaiserslautern, for his support.

REFERENCES

[1] Abaqus inc. http://www.abaqus.com/.

[2] Ansys. http://www.ansys.com/.

[3] P. A. Cundall. A discontinuous future for numerical modeling in soil and rock. In B. K. Cook and R. P. Jensen, editors, *Discrete Element Methods, Numerical Modeling of Discontinua , Proceedings of the 3rd International Conference on Discrete Element Methods*, pages 3–4. ASCE American Society of Civil Engineers, 2002.

[4] P. A. Cundall and O. D. L. Strack. The distinct element method as a tool for research in granular media. *Report to the National Science Foundation Concerning NSF Grant ENG76-20711, PART I*, 1978.

[5] P. A. Cundall and O. D. L. Strack. A discrete numerical model for granular assemblies. *Géotechnique*, 29(1):47–65, 1979.

[6] P. A. Cundall and O. D. L. Strack. The distinct element method as a tool for research in granular media. *Report to the National Science Foundation Concerning NSF Grant ENG76-20711, PART II*, 1979.

[7] W. Day and H. Edelsbrunner. Efficient algorithms for agglomerative hierarchical clustering methods. *Journal of Classification*, 1(1):7–24, 1984.

[8] M. de Berg, M. van Kreveld, M. Overmars, and O. Schwarzkopf. *Computational Geometry: Algorithms and Applications*. Springer-Verlag, Jan. 2000.

[9] D. Defays. An efficient algorithm for a complete link method. *The Computer Journal*, 20(4):364–366, 1977.

[10] Dem solutions. http://www.dem-solutions.com/demsolutions.html.

[11] S. Fortune. A sweepline algorithm for Voronoi diagrams. *Algorithmica*, 2:153–174, 1987.

[12] J. F. Hair, R. E. Anderson, R. L. Tatham, and Black. *Multivariate Data Analysis*. Prentice Hall College Div, 2006.

[13] R. Hill. On constitutive macro-variables for heterogeneous solids at finite strain. *Proc. R. Soc. Lond. A*, 326:131–147, 1972.

[14] Itasca consultants gmbh. http://www.itasca.de/.

[15] L. E. Malvern. *Introduction to the Mechanics of a Continuous Medium*. Prentice-Hall, 1969.

[16] H. A. Meier, E. Kuhl, and P. Steinmann. A note on the generation of periodic granular microstructures based on grain size distributions. *Submitted for publication*, 2006.

[17] S. Nemat-Nasser. Averaging theorems in finite deformation plasticity. *Mechanics of Materials*, 31:493–523, 1999.

[18] F. Nightingale. *Notes on Matters Affecting the Health, Efficiency, and Hospital Administration of the British Army*. London: Harrison & Sons., 1858.

[19] J. H. Ward, Jr. Hierarchical grouping to optimize an objective function. *Journal of the American Statistical Association*, 58:236–244, 1963.

[20] T. I. Zohdi and P. Wriggers. *Introduction to computational micromechanics*. Springer-Verlag, 2005.